Sun-Believable Solar Paint. A Transformative One-Step Approach for Designing Nanocrystalline Solar Cells

Matthew P. Genovese,[†] Ian V. Lightcap, and Prashant V. Kamat*

Radiation Laboratory and Department of Chemistry and Biochemistry, University of Notre Dame, Notre Dame, Indiana 46556, United States [†]Coop Student, University of Waterloo, Canada.

ABSTRACT

A transformative approach is required to meet the demand of economically viable solar cell technology. By making use of recent advances in semiconductor nanocrystal research, we have now developed a one-coat solar paint for designing quantum dot solar cells. A binder-free paste consisting of CdS, CdSe, and TiO_2 semiconductor nanoparticles was prepared and applied to conducting glass surface and annealed at 473 K. The photoconversion behavior of these semiconductor film electrodes was evaluated in a photoelectrochemical cell consisting of graphene—Cu_2S counter electrode and sulfide/polysulfide redox couple. Open-circuit voltage as high as 600 mV and short circuit current of 3.1 mA/cm^2 were obtained with CdS/TiO_2—CdSe/TiO_2 electrodes. A power conversion efficiency exceeding 1% has been obtained for solar cells constructed using the simple conventional paint brush approach under ambient conditions. Whereas further improvements are necessary to develop strategies for large area, all solid state devices, this initial effort to prepare solar paint offers the advantages of simple design and economically viable next generation solar cells.

KEYWORDS: solar cells · photoconversion · solar paint · semiconductor nanocrystals · photoelectrochemistry · metal chalcogenides

What if all it takes is a coat of paint to convert light energy into electricity? That is the challenge that needs to be addressed if we desire to have a transformative photovoltaic technology and meet future energy needs.[1,2] In recent years semiconductor nanocrystal or quantum-dot-based solar cells have drawn significant attention as viable candidates for boosting the energy conversion efficiency beyond the traditional Shockley and Queisser limit of 32% for Si-based solar cells.[3−12]

Because of the extremely small size of semiconductor quantum dots and high absorption cross section, it is possible to capture nearly all of the incident solar light in the visible region with an extremely thin layer of semiconductor materials. These heterojunction semiconductor solar cells, often referred as ETA (extremely thin absorber) cells, offer new opportunities to develop relatively inexpensive solar cells.[13,14] One such example utilizes a PbS and TiO_2 heterojunction and is reported to exhibit a power conversion efficiency of 5.1%.[15] Similarly, Sb_2S_3-based ETA solar cells have delivered efficiencies greater than 5%.[13,16,17] These recent developments of photoinduced charge separation using semiconductor nanocrystal-based assemblies and efforts to utilize them in solar cells paves the way to propose transformative research efforts.

The other type of quantum dot solar cell employs metal chalcogenide semiconductors as sensitizers which, upon excitation, inject electrons into large band gap semiconductors such as TiO_2. The sulfide/polysulfide redox couple, which scavenges holes from the photoanode, is regenerated at the counter electrode. The photoelectrochemical cells employing CdS and CdSe have been widely studied, and power conversion efficiency in the 3−4% range is often achieved.[14−16,18−22] A recent study that overcomes the redox limitation at the counter electrode by using Cu_2S/reduced graphene oxide has produced efficiency as high as 4.4%.[22] Previous work in our laboratory has provided understanding of the photoinduced charge transfer processes in semiconductor quantum dots and their utilization in semiconductor-sensitized solar cells (Scheme 1).[23−25]

* Address correspondence to pkamat@nd.edu.

Received for review November 11, 2011 and accepted December 6, 2011.

Published online December 06, 2011
10.1021/nn204381g

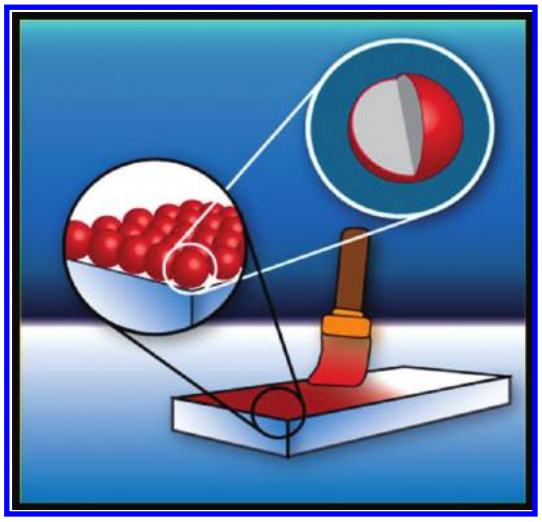

Scheme 1. Schematic illustrating the principle of the solar paint approach. TiO_2 nanoparticles are coated with CdS or CdSe *via* a pseudo-SILAR method. These composite particles are applied in a paint-like, one-step photoanode formation.

Both types of cells discussed above utilize a series of sequential deposition steps to attain a better performing photoanode. Completing the full range of semiconductor film deposition and annealing protocols is time-intensive, requiring multiple steps and 1 or 2 days to attain the best performing cells. In order to produce more versatile and economically viable quantum dot solar cells, it is important to simplify the electrode preparation procedures. One of the earliest attempts to simplify construction of photoelectrochemical cells using a paint approach was made by Hodes and coworkers.[26] They employed a polycrystalline powder CdSe and CdTe with a fluxing material such as $CdCl_2$ and sintered at ~650 °C.[26] With the recent advances in semiconductor-sensitized solar cells, we have now prepared solar paint consisting of CdS, CdSe, and TiO_2 nanoparticles. A one-step coating approach to design relatively high efficiency semiconductor-sensitized solar cells is described.

Preparation of Solar Paint. We adopted two synthetic strategies: (1) physical mixing of commercially available TiO_2 (Degussa P25) and bulk CdS (Aldrich) in a mixed solvent (water and *t*-butanol); (2) a pseudo-SILAR (sequential ionic layer adsorption and reaction) method of depositing CdS (or CdSe) on suspended TiO_2 nanoparticles by the addition of Cd^{2+} and S^{2-} (or Se^{2-}) in a stepwise fashion. In addition, we also included ZnO powder with TiO_2 before mixing with CdS so that any beneficial aspects due to charge separation in the ZnO−TiO_2 composite semiconductor can be tested. Procedural details are presented in the Experimental Methods. The resulting thick, yellow paste of TiO_2 and CdS could then be applied directly on conducting glass electrodes. The photographs in Figure 1 show the preparation steps of solar paint by direct mixing of the solvent with preformed particles (A,B) and SILAR method (C,D). The photograph E in Figure 1 shows the application of the paint to an optically transparent electrode (OTE), and photographs F−H show the examples of electrodes after the low-temperature annealing procedure. TiO_2/CdS and TiO_2/CdSe electrodes in Figure 2F−H were prepared using pseudo-SILAR procedure. These electrodes were further subjected to the evaluation of photoelectrochemical performance.

RESULTS/DISCUSSION

Figure 2A shows the absorption spectra of electrodes prepared with mixed CdS/TiO_2, SILAR CdS/TiO_2, and SILAR CdSe/TiO_2. The absorption onset seen in these spectra around ~550 and 680 nm is characteristic of CdS and CdSe, respectively. An electrode was also prepared using a mixture of SILAR CdS and CdSe, 1.5:1.0 wt %, deposited on TiO_2 nanoparticles. Spectrum (c) shows the overlap of absorption arising from CdS and CdSe nanoparticles. The relatively high absorbance seen in the visible shows the strong absorption properties of solar paint. More details on the role of semiconductor nanoparticles as extremely thin absorbers (ETA) in solar cell applications have been discussed in earlier studies.[13,16,17]

The morphology of solar paint mixtures was analyzed using scanning and transmission electron microscopy (SEM and TEM). The SEM image in Figure 2B reveals two size regimes for CdSe: sub-10 nm diameter nanoparticles and larger 1−6 μm sized particles. The smaller nanoparticles result from SILAR seeding of CdSe on the TiO_2 surface, whereas the larger particles are most likely formed by precipitation of bulk CdSe in solution along with subsequent physical mixing with TiO_2 nanoparticles (20−50 nm diameter). The absorbance spectra for composites formed *via* the pseudo-SILAR process confirm the presence of bulk CdS and CdSe in these composites. High-resolution TEM was also utilized to analyze local solar paint morphology and confirms the attachment of CdSe nanoparticles to TiO_2 (Figure 2C). Lattice spacings highlighted in the image show *d*-spacings of 0.215 nm, characteristic of the (110) face of wurtzite CdSe. Also shown are 0.352 nm spacings which correspond to the (101) face for anatase TiO_2.

Photoelectrochemical Characterization of Films Prepared by Mixing TiO_2 and CdS Nanoparticles. The electrodes prepared using solar paint were evaluated in a photoelectrochemical cell consisting of semiconductor film photoanode, Cu_2S-reduced graphene oxide counter electrode, and sulfide/polysulfide electrolyte (1 M/1 M).[22] A series of experiments were carried out in a sandwich cell configuration to optimize the ratio of CdS and TiO_2 in the solar paint. The *I*−*V* characteristics under 100 mW/cm^2, AM 1.5 solar irradiation for three different compositions of CdS/TiO_2 are shown in Figure 3A. Fill factors obtained from the *I*−*V* curves are in the range of 0.51−0.55. The CdS/TiO_2 films also show

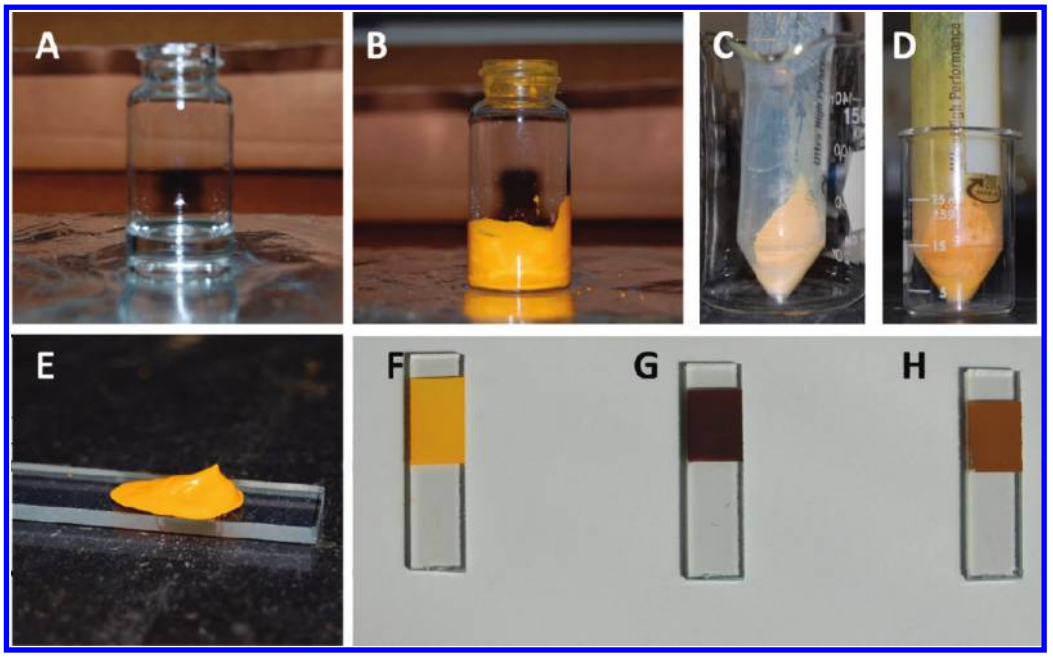

Figure 1. (A) *tert*-Butanol and water are used as solvent. (B) Bulk CdS powder and TiO_2 powder are slowly mixed into the solvent, forming solar paint. (C,D) CdS deposited on TiO_2 after 1 and 8 cycles of pseudo-SILAR process, respectively. (E) Application of solar paint to an OTE (optically transparent electrode). (F–H) Annealed films of solar paint: (F) CdS/TiO_2 (8 SILAR cycles), (G) CdSe/TiO_2 (3 SILAR cycles) films, and (H) mixture of F,G.

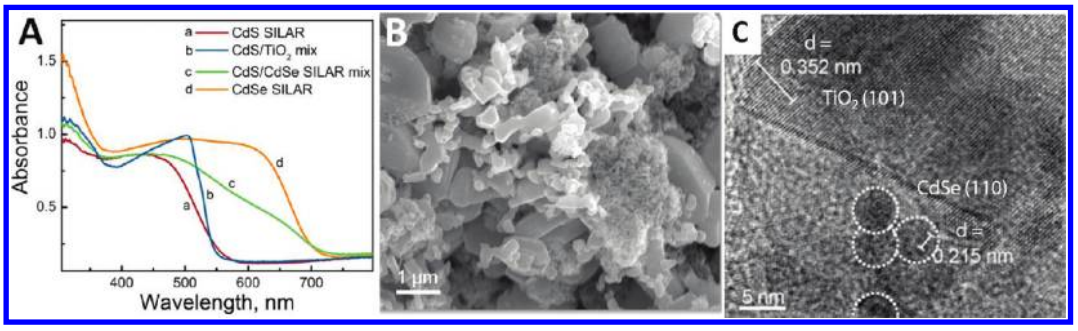

Figure 2. (A) Absorbance traces shown for solar paints made from (a) SILAR CdS/TiO_2, (b) CdS powder mixed with TiO_2, (c) SILAR CdS/TiO_2 mixed with CdSe/TiO_2, and (d) SILAR CdSe/TiO_2. All films were annealed at 200 °C. (B) SEM image shows SILAR CdSe on TiO_2. (C) High-resolution TEM shows CdSe nanoparticles with a ~4 nm diameter on TiO_2 ($d \sim 40$ nm). Lattice spacings of 0.215 nm for the CdSe (110) plane and 0.352 nm for the TiO_2 (101) plane confirm the nature of the composite. Dotted lines serve to guide reader's eye to CdSe nanoparticle edges.

prompt current response to illumination with short circuit currents in the range of 2.0–2.3 mA/cm^2 (Figure 3B). The results of three representative compositions show that the ratio of 1.5:1.0 CdS/TiO_2 is optimal for achieving maximum photocurrent generation. It is interesting to note that the open circuit potential of all three electrodes were around 600 mV, unaffected by the ratio of CdS/TiO_2. If we exclude TiO_2 from the paste, the performance of the solar paint gave poor performance. Films made from CdS alone result in a short circuit current of ~80 μA/cm^2 and a V_{oc} of ~0.27 V.

We also prepared solar paint using mixed ZnO and CdS nanoparticles. Similar photoelectrochemical performance was observed with CdS/ZnO paint, albeit with fill factors in the range of 0.24–0.35. Under prolonged illumination, some photocurrent decay is observed in these composites and is attributed to the reaction with ZnO and S^{2-} to produce ZnS (see Supporting Information, Figure S1). The stability of the CdS/ZnO paints is significantly improved by the addition of TiO_2 to the composites. Figure 3C shows short circuit currents between 3.0 and 3.5 mA/cm^2 for CdS/ZnO/TiO_2 composites with varying amounts of TiO_2. The I–V curves for the CdS/ZnO/TiO_2 paints gave fill factors in the range of 0.36–0.39 (see Supporting Information, Figure S2).

As discussed in earlier studies,[4,14,27,28] the difference between apparent Fermi level of the photoanode and the redox equilibration potential of the counter electrode dictates the open circuit potential of a photoelectrochemical cell. The results presented in Figure 3 highlight the ability to deliver maximum photopotential without undergoing losses.

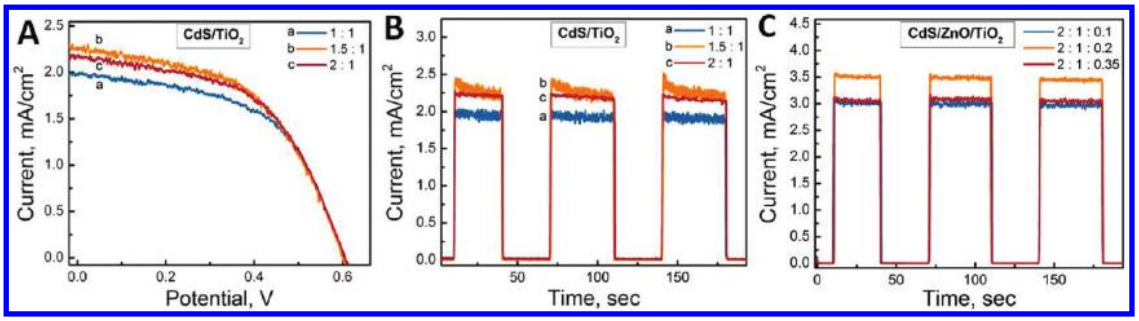

Figure 3. (A) *I*–*V* curves for solar paints composed of different CdS/TiO_2 mass ratios (mixed powders) as photoanodes. (B) Current–time plots for those films show prompt current response of solar paint to illumination. (C) Current–time plots for CdS/ZnO/TiO_2 paints with varying amounts of TiO_2 exhibit increased photocurrent over CdS/TiO_2 paints. All films were tested under 100 mW/cm^2, AM 1.5 irradiation with a Cu_2S-reduced graphene oxide counter electrode and Na_2S/S electrolyte.

In most studies involving quantum-dot-sensitized solar cells (QDSC), one constructs the photoactive electrode by first depositing mesoscopic films that are later modified with metal chalcogenide (*e.g.*, CdS or CdSe) nanocrystals.[4,29] Both molecular linked approach[30,31] and SILAR[32–36] have been successfully employed to attach an extremely thin layer of metal chalcogenide to the TiO_2 film. Upon excitation of CdS (or CdSe), the electrons are injected into TiO_2 nanoparticles. The electrons then travel through the network of TiO_2 nanoparticles and are collected by the conducting electrode surface. The redox couple present in the electrolyte (usually sulfide/polysulfide) scavenges holes at the photoanode and is then regenerated at the counter electrode.

$$\mathrm{CdS} + h\nu \rightarrow \mathrm{CdS(e + h)} \quad (1)$$

$$\mathrm{CdS(e)} + \mathrm{TiO_2} \rightarrow \mathrm{CdS} + \mathrm{TiO_2(e)} \quad (2)$$

$$\mathrm{CdS(h)} + \mathrm{S^{2-}} \rightarrow \mathrm{CdS} + \mathrm{S^{-\bullet}} \quad (3)$$

The electron injection into TiO_2 and hole scavenging by sulfide kinetics are the primary processes that dictate the overall photocurrent generation efficiency. As pointed out in our earlier studies, the charge injection process (reaction 2) which occurs with a rate constant of 10^{10}–10^{11} s^{-1} can be modulated by varying the size of the metal chalcogenide nanoparticles.[24] Despite this fast electron injection into TiO_2 nanoparticles, a major bottleneck arises from the slower hole scavenging rate ($k \sim 10^8$ s^{-1}).[25] In addition, back electron transfer with the oxidized form of the redox couple and the inefficient response of the counter electrode have been identified as key factors limiting the efficiency of QDSC.

The solar paint prepared in this study lacks a well-defined ordered structure. The SEM image shown in Figure 2B indicates that there are clusters of TiO_2 and CdSe nanoparticles in the microdomain of the film. Despite our effort to achieve uniform mixing through sonication, the aggregated particle network exists in the film. The fact that we observe deliverance of good photoelectrochemical performance of solar paint suggests the ability of CdSe and TiO_2 microclusters to interact and attain good charge separation.

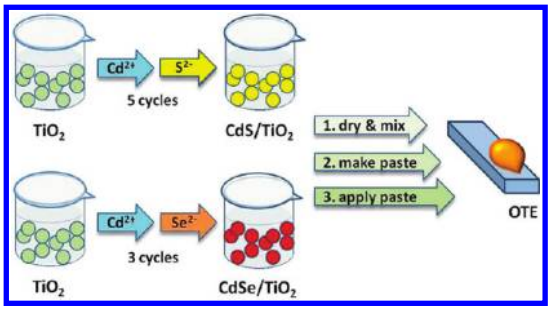

Scheme 2. Pseudo-SILAR method of depositing sequential layers of CdS and CdSe on suspended TiO_2 nanoparticles. For CdS/TiO_2 (or CdSe/TiO_2), the procedure involved a single step of 8 repeat cycles of Cd^{2+} and S^{2-} (or 3 repeat cycles of Cd^{2+} and Se^{2-}) addition. All particles were subjected to the capping of ZnS through the addition of Zn^{2+} and S^{2-} (not shown).

Photoelectrochemical Performance of Solar Paint Prepared Using Pseudo-SILAR Approach. In order to establish a close contact between TiO_2 and metal chalcogenide nanostructures, we modified the conventional SILAR method by precipitating CdS and CdSe in a suspension of TiO_2 nanoparticles. As described in the Experimental Methods, Cd^{2+} and S^{2-} (or Se^{2-}) precursor solutions were sequentially added to a stirred TiO_2 suspension (Scheme 2). This method facilitated direct deposition of CdS (or CdSe) on TiO_2 nanoparticles. During the last step, 10 mL of 0.1 M of $Zn(C_2H_3O_2)_2$ solution was added to the composite nanoparticles and then centrifuged. This was followed by a final treatment of S^{2-} (10 mL of 0.1 M Na_2S) to give a thin layer of ZnS. Earlier studies have shown improved photoelectrochemical performance using a ZnS coating as it serves as a barrier for the charge recombination process.[19] The composites were prepared as a paste and applied to the conducting, fluorine-doped tin oxide (FTO) surface of an OTE and tested individually as well as in a mixed form.

Figure 4 shows the photocurrent action spectra of three electrodes prepared by pseudo-SILAR approach. The incident photon to current conversion efficiencies

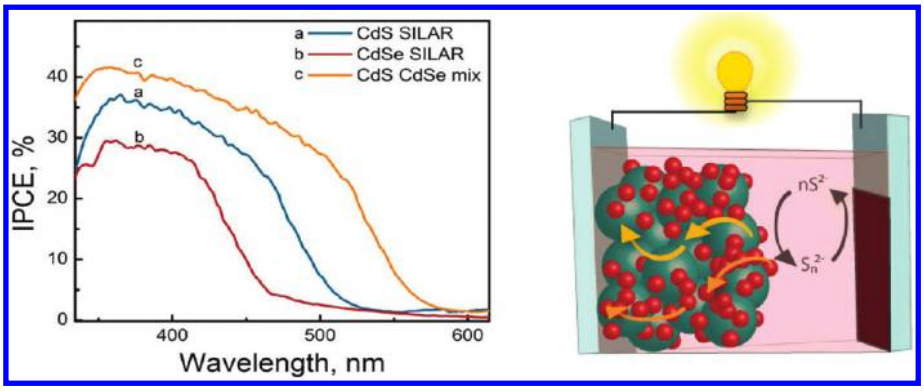

Figure 4. Left: Photocurrent response of (a) CdS/TiO_2, (b) CdSe/TiO_2, and (c) CdSe/CdS/TiO_2 electrodes as monitored from the IPCE at different wavelength of irradiation (counter electrode, reduced graphene oxide/Cu_2S film deposited on OTE; and electrolyte, 1 M Na_2S and 1 M S in water). Right: Schematic illustration of photocurrent generation depicting the electron transport through the network of TiO_2 clusters (yellow arrow) and CdS (or CdSe) cluster network (orange arrow).

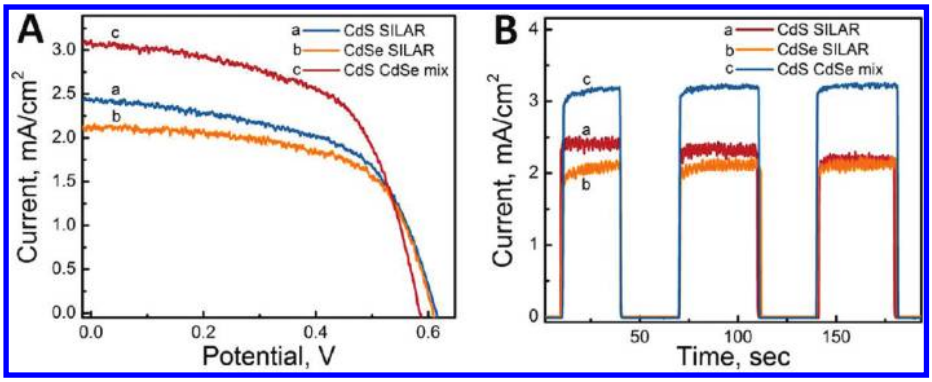

Figure 5. (A) *I*−*V* curves for solar paints formed with the pseudo-SILAR deposition process. The mixed CdS/TiO_2−CdSe/TiO_2 paint outperforms paints composed of only CdS/TiO_2 or CdSe/TiO_2. (B) Current−time plots for paints show prompt photocurrent response.

at different wavelengths were determined from the short circuit current (I_{sc}) and incident light intensity (P_{inc}) at incident wavelength, λ (nm)

$$\text{IPCE}(\%) = (1240/\lambda) \times (I_{sc}/P_{inc}) \times 100 \qquad (4)$$

It is interesting to note that all three electrodes exhibit photocurrent generation efficiency in the range of 30−40%. The photoresponse of the CdS/TiO_2 electrode shows an onset of photocurrent generation at 525 nm, confirming thereby the response to arise from the band gap excitation of the CdS nanoparticles. TiO_2/CdSe on the other hand exhibits relatively poor response in the visible with more noticeable trend above 460 nm. Because of the smaller band gap of CdSe, we would have expected to see a good response up to 680 nm (see absorption spectra in Figure 1). The minimal photoresponse seen for the TiO_2/CdSe film at wavelengths greater than 460 nm is attributed to a movement by the CdSe conduction band edge to more positive potentials as a result of crystalline growth to bulk values. This, in turn, hinders excited state electron injection into the TiO_2 conduction band due to a loss in driving force. However, the composite films of CdS and CdSe deposited on TiO_2 exhibit an extended response in the visible with an onset at 600 nm. Intimate contact between CdS and CdSe in these films under illumination should result in band-filling leading to pseudo-Fermi level equilibration of conduction bands. This would re-establish the CdSe conduction band to more negative potentials and restore the driving force for excited state electron injection. These results point out the synergy of CdS and CdSe in utilizing incident visible photons and thus delivering higher IPCE.

I−*V* characteristics and photocurrent response of CdS/TiO_2, CdSe/TiO_2, and CdS/TiO_2−CdSe/TiO_2 electrodes under AM 1.5 light irradiation are shown in Figure 5, and the cell parameters are compared in Table 1. The solar paint prepared by pseudo-SILAR method exhibits prompt photocurrent response in the range of 2−3 mA/cm^2 and an open circuit voltage in the range of 585−615 mV. The fill factor for these cells was found to be around 0.6, suggesting superior electrochemical performance. The composite of mixed CdS/TiO_2 and CdSe/TiO_2 nanoparticles achieved the best performance with a power conversion efficiency exceeding 1%.

Sensitization of TiO_2 by excited CdS and CdSe has been well studied.[4,27,37−41] In quantum-dot-sensitized

TABLE 1. Photoelectrochemical Performance of Solar Paints[a]

electrode	ratio	method	J_{sc} (mA/cm^2)	V_{oc} (mV)	FF	η (%)
CdS/TiO_2	1.5:1.0	mix	2.26	600	0.52	0.71
CdS/ZnO	2.25:1.0	mix	3.01	675	0.28	0.57
CdS/ZnO/TiO_2	2.0:1.0:0.2	mix	3.63	685	0.36	0.89
CdS/TiO_2	1.0:3.5	SILAR	2.33	615	0.61	0.87
CdSe/TiO_2	1.0:5.0	SILAR	2.12	608	0.64	0.83
CdS—TiO_2/CdSe—TiO_2	1.0:1.5	SILAR, mix	3.1	585	0.59	1.08

[a] Sandwich cell configuration. Electrolyte = 1 M Na_2S/1 M S in water; counter electrode, Cu_2S/RGO composite film on OTE, AM 1.5 sunlight illumination. Active electrode area 0.15—0.2 cm^2.

solar cells, the initial charge separation at the TiO_2 interface is the primary step following the band gap excitation of CdS (or CdSe). The scavenging of holes by S^{2-} results in accumulation of electrons in the semiconductor film. The accumulation of electrons drives the Fermi level to more negative potential as noted from the steady photovoltage. Upon application of load, the accumulated electrons are transported *via* the TiO_2 and CdS (or CdSe) nanoparticle network to the collecting electrode surface. The two routes of electron transport within the nanostructured film are illustrated in Figure 4.

The photoelectrochemical results presented in Table 1 compare and contrast the behavior of solar cells constructed using solar paints prepared with different strategies. While simple mixing of TiO_2 and CdS powders in the form of a paint can deliver power conversion efficiency of about 0.8%, we can further improve the efficiency by depositing CdS and/or CdSe directly on TiO_2 nanoparticles. The merit of the present study lies in the utilization of semiconductor sensitization aspect with a simple and versatile approach. Even the annealing step can be simplified by subjecting the films to hot air. One such experimental arrangement we tested to anneal semiconductor films at 120 °C using a hot air blower is shown in the Supporting Information. The cells prepared using hot air annealing of semiconductor films also performed quite well with efficiency in the range of 0.5—0.8%.

CONCLUSION

The highest efficiency of >1% for QDSC cells prepared using the solar paint approach is nearly five times lower than the highest recorded efficiency for SILAR-based QDSC prepared by multifilm architecture of mesoscopic TiO_2 layers (*viz.*, compact layer, adsorber layer, and scattering layer) followed by careful layering of CdS or CdSe. The latter approach can take up to a day or two to prepare photoactive anodes. On the other hand, the solar paint offers the convenience of a one-step photoactive layer application on the electrode surface with electrode preparation time of less than an hour. Obviously, further optimization and use of different semiconductor nanoparticles are necessary to boost the efficiency of such solar cells. The present work of designing *Sun-Believable solar paint* is a first step toward the development of a transformative technology for the construction of nanocrystalline semiconductor-based solar cells.

EXPERIMENTAL METHODS

Materials. Zinc oxide ultrapure (electronic grade), sulfur powder (325 mesh 99.5%), cadmium nitrate tetrahydrate (98.5%), and selenium(IV) oxide (99.4%, metal basis) were obtained from Alfa Aesar. Tertiary butyl alcohol (certified), 1 methyl-2-pyrrolidinone, and Versa Clean solution were obtained from Fisher Scientific. Cadmium sulfide powder (99.999%, trace metal basis) and sodium sulfide nonahydrate (98%) were obtained from Sigma Aldrich. Cadmium sulfate anhydrous (99.7%) was obtained from J.T. Baker Scientific. Sodium borohydride 98% was obtained from Stern Chemicals. Titanium dioxide, P25, was obtained from Degussa.

CdS/TiO_2 Mixed Paint. The preparation of binder-free CdS/TiO_2 paste was adapted from a previous report.[42] Briefly, CdS powder (0.5 g) was mixed into 3 mL of *tert*-butyl alcohol/water (2:1 volume) solvent. TiO_2 powder (0.5 g) was slowly added with mixing and under gentle heating (~40 °C). The range of CdS/TiO_2 ratios tested is reported above. ZnO (0.5 g)/CdS (0.75—1.5 g) pastes were prepared similarly.

Pseudo-SILAR CdS/TiO_2 and CdSe/TiO_2 Paints. The pseudo-SILAR CdS/TiO_2 and CdSe/TiO_2 paints were prepared by suspending TiO_2 (0.5 g) in 15 mL of water/methanol (3:1 volume) using gentle sonication. After suspension, 100 μL of 0.1 M NaOH was added to the TiO_2 slurry. Next, 2 mL of 0.1 M $CdSO_4$ in water/methanol (1:1) was added and mixed for ~30 s before addition of 2 mL of 0.1 M Na_2S in water/methanol (1:1) (or 0.1 M SeO_2, which was reduced in an oxygen-free environment with 2 equiv of $NaBH_4$) followed by additional mixing for another 30 s. The mixture was centrifuged (7000 rpm), supernatant discarded, and the solid CdS/TiO_2 resuspended. This cycle was repeated 8 times for CdS/TiO_2 and 3 times for CdSe/TiO_2 composites. The solid product was then dried with typical yields of ~700 mg.

Solar paint from the pseudo-SILAR process was prepared using the method mentioned above for mixed CdS/TiO_2 paints, with additions of ~1 g of the SILAR products CdS/TiO_2 or CdSe/TiO_2 to the *tert*-butyl alcohol/water solvent. A paint was also made using a mixture of SILAR CdS/TiO_2 (~400 mg) and CdSe/TiO_2 (~605 mg).

Cell Construction. For the photoanode, fluorine-doped tin oxide electrodes were pretreated with $TiCl_4$ (40 mM, 70 °C for 30 min). Paints were applied *via* a doctor blade method to fluorine-doped tin oxide electrodes and annealed under nitrogen for 60 min at 200 °C. The counter electrode utilized a Cu_2S—graphene composite, the construction of which is described in a previous report.[22] A mixture of 1 M sodium sulfide and 1 M sulfur was employed as the electrolyte. Cells were configured in a sandwich cell orientation with a Parafilm spacer.

Optical, Photoelectrochemical, and Structural Characterization. Diffuse reflectance absorption spectra were recorded using a Shimadzu UV-3101PC spectrophotometer. Photoelectrochemical measurements were conducted using a Princeton Applied Research Potentiostat 2263 in a two electrode, sandwich cell configuration. Active areas for cells tested were in the range of 0.15—0.20 cm^2. A 300 W xenon lamp with an AM 1.5 filter was used as the excitation source. A Newport Oriel QE/IPCE measurement kit was employed for IPCE measurements. SEM images were made using a FEI Magellen-400 FESEM. TEM micrographs were taken using FEI Titan 300 kV field emission TEM with Gatan image filter.

Acknowledgment. The research described herein was supported by the Division of Chemical Sciences, Geosciences, and Biosciences, Office of Basic Energy Sciences of the U.S. Department of Energy through award DE-FC02-04ER15533. We would like to thank Hyunbong Choi and Praly Santra for helpful discussions. This is contribution number NDRL 4904 from the Notre Dame Radiation Laboratory.

Supporting Information Available: Additional *I*–*V* characteristics, current–time profiles, and hot air annealing arrangements are presented. This material is available free of charge *via* the Internet at http://pubs.acs.org.

REFERENCES AND NOTES

1. Kamat, P. V. Meeting the Clean Energy Demand: Nanostructure Architectures for Solar Energy Conversion. *J. Phys. Chem. C* **2007**, *111*, 2834–2860.
2. Lewis, N. S.; Nocera, D. G. Powering the Planet: Chemical Challenges in Solar Energy Utilization. *Proc. Natl. Acad. Sci. U.S.A.* **2006**, *103*, 15729–15735.
3. Shockley, W.; Queisser, H. J. Detailed Balance Limit of Efficiency of p–n Junction Solar Cells. *J. Appl. Phys.* **1961**, *32*, 510–519.
4. Kamat, P. V.; Tvrdy, K.; Baker, D. R.; Radich, J. G. Beyond Photovoltaics: Semiconductor Nanoarchitectures for Liquid Junction Solar Cells. *Chem. Rev.* **2010**, *110*, 6664–6688.
5. Mora-Sero, I.; Bisquert, J. Breakthroughs in the Development of Semiconductor Sensitized Solar Cells. *J. Phys. Chem. Lett.* **2010**, *1*, 3046–3052.
6. Buhbut, S.; Itzhakov, S.; Oron, D.; Zaban, A. Quantum Dot Antennas for Photoelectrochemical Solar Cells. *J. Phys. Chem. Lett.* **2011**, *2*, 1917–1924.
7. Hetsch, F.; Xu, X.; Wang, H.; Kershaw, S. V.; Rogach, A. L. Semiconductor Nanocrystal Quantum Dots as Solar Cell Components and Photosensitizers: Material, Charge Transfer, and Separation Aspects of Some Device Topologies. *J. Phys. Chem. Lett.* **2011**, *2*, 1879–1887.
8. Nozik, A. J.; Beard, M. C.; Luther, J. M.; Law, M.; Ellingson, R. J.; Johnson, J. C. Semiconductor Quantum Dots and Quantum Dot Arrays and Applications of Multiple Exciton Generation to Third-Generation Photovoltaic Solar Cells. *Chem. Rev.* **2010**, *110*, 6873–6890.
9. Beard, M. C. Multiple Exciton Generation in Semiconductor Quantum Dots. *J. Phys. Chem. Lett.* **2011**, *2*, 1282–1288.
10. Choi, J. J.; Lim, Y.-F.; Santiago-Berrios, M. E. B.; Oh, M.; Hyun, B.-R.; Sun, L.; Bartnik, A. C.; Goedhart, A.; Malliaras, G. G.; Abruna, H. D.; *et al.* PbSe Nanocrystal Excitonic Solar Cells. *Nano Lett.* **2009**, *9*, 3749–3755.
11. Buhbut, S.; Itzhakov, S.; Tauber, E.; Shalom, M.; Hod, I.; Geiger, T.; Garini, Y.; Oron, D.; Zaban, A. Built-in Quantum Dot Antennas in Dye-Sensitized Solar Cells. *ACS Nano* **2010**, *4*, 1293–1298.
12. Zhang, Q. X.; Guo, X. Z.; Huang, X. M.; Huang, S. Q.; Luo, Y. H.; Shen, Q.; Toyoda, T.; Meng, Q. B.; Li, D. M. Highly Efficient CdS/CdSe-Sensitized Solar Cells Controlled by the Structural Properties of Compact Porous TiO_2 Photoelectrodes. *Phys. Chem. Chem. Phys.* **2011**, *13*, 4659–4667.
13. Itzhaik, Y.; Niitsoo, O.; Page, M.; Hodes, G. Sb_2S_3-Sensitized Nanoporous TiO_2 Solar Cells. *J. Phys. Chem. C* **2009**, *113*, 4254–4256.
14. Gonzalez-Pedro, V.; Xu, X.; Mora-Sero, I.; Bisquert, J. Modeling High-Efficiency Quantum Dot Sensitized Solar Cells. *ACS Nano* **2010**, *4*, 5783–5790.
15. Pattantyus-Abraham, A. G.; Kramer, I. J.; Barkhouse, A. R.; Wang, X.; Konstantatos, G.; Debnath, R.; Levina, L.; Raabe, I.; Nazeeruddin, M. K.; Grätzel, M.; *et al.* Depleted-Heterojunction Colloidal Quantum Dot Solar Cells. *ACS Nano* **2010**, *4*, 3374–3380.
16. Chang, J. A.; Rhee, J. H.; Im, S. H.; Lee, Y. H.; Kim, H.-j.; Seok, S. I.; Nazeeruddin, M. K.; Gratzel, M. High-Performance Nanostructured Inorganic–Organic Heterojunction Solar Cells. *Nano Lett.* **2010**, *10*, 2609–2612.
17. Moon, S.-J.; Itzhaik, Y.; Yum, J.-H.; Zakeeruddin, S. M.; Hodes, G.; Gratzel, M. Sb_2S_3-Based Mesoscopic Solar Cell Using an Organic Hole Conductor. *J. Phys. Chem. Lett.* **2010**, *1*, 1524–1527.
18. Diguna, L. J.; Shen, Q.; Kobayashi, J.; Toyoda, T. High Efficiency of CdSe Quantum-Dot-Sensitized TiO_2 Inverse Opal Solar Cells. *Appl. Phys. Lett.* **2007**, *91*, 023116.
19. Shen, Q.; Kobayashi, J.; Diguna, L. J.; Toyoda, T. Effect of ZnS Coating on the Photovoltaic Properties of CdSe Quantum Dot-Sensitized Solar Cells. *J. Appl. Phys.* **2008**, *103*, 084304.
20. Barea, E. M.; Shalom, M.; Giménez, S.; Hod, I.; Mora-Seró, I. N.; Zaban, A.; Bisquert, J. Design of Injection and Recombination in Quantum Dot Sensitized Solar Cells. *J. Am. Chem. Soc.* **2010**, *132*, 6834–6839.
21. Liu, L.; Hensel, J.; Fitzmorris, R. C.; Li, Y.; Zhang, J. Z. Preparation and Photoelectrochemical Properties of CdSe/TiO2 Hybrid Mesoporous Structures. *J. Phys. Chem. Lett.* **2010**, *1*, 155–160.
22. Radich, J. G.; Dwyer, R.; Kamat, P. V. Cu_2S-Reduced Graphene Oxide Composite for High Efficiency Quantum Dot Solar Cells. Overcoming the Redox Limitations of S^{2-}/S_n^{2-} at the Counter Electrode. *J. Phys. Chem. Lett.* **2011**, *2*, 2453–2460.
23. Bang, J. H.; Kamat, P. V. Quantum Dot Sensitized Solar Cells. A Tale of Two Semiconductor Nanocrystals: CdSe and CdTe. *ACS Nano* **2009**, *3*, 1467–1476.
24. Tvrdy, K.; Frantszov, P.; Kamat, P. V. Photoinduced Electron Transfer from Semiconductor Quantum Dots to Metal Oxide Nanoparticles. *Proc. Natl. Acad. Sci. U.S.A.* **2011**, *108*, 29–34.
25. Chakrapani, V.; Baker, D.; Kamat, P. V. Understanding the Role of the Sulfide Redox Couple (S^{2-}/S_n^{2-}) in Quantum Dot Sensitized Solar Cells. *J. Am. Chem. Soc.* **2011**, *133*, 9607–9615.
26. Hodes, G.; Cahen, D.; Manassen, J.; David, M. Painted, Polycrystalline Thin Film Photoelectrodes for Photoelectrochemical Solar Cells. *J. Electrochem. Soc.* **1980**, *127*, 2252–2254.
27. Hodes, G. Comparison of Dye- and Semiconductor-Sensitized Porous Nanocrystalline Liquid Junction Solar Cells. *J. Phys. Chem. C* **2008**, *112*, 17778–17787.
28. Bisquert, J.; Garcia-Belmonte, G. On Voltage, Photovoltage, and Photocurrent in Bulk Heterojunction Organic Solar Cells. *J. Phys. Chem. Lett.* **2011**, *2*, 1950–1964.
29. Kamat, P. V. Quantum Dot Solar Cells. Semiconductor Nanocrystals as Light Harvesters. *J. Phys. Chem. C* **2008**, *112*, 18737–18753.
30. Robel, I.; Subramanian, V.; Kuno, M.; Kamat, P. V. Quantum Dot Solar Cells. Harvesting Light Energy with CdSe Nanocrystals Molecularly Linked to Mesoscopic TiO_2 Films. *J. Am. Chem. Soc.* **2006**, *128*, 2385–2393.
31. Watson, D. F. Linker-Assisted Assembly and Interfacial Electron-Transfer Reactivity of Quantum Dota Substrate Architectures. *J. Phys. Chem. Lett.* **2010**, *1*, 2299–2309.
32. Baker, D. R.; Kamat, P. V. Photosensitization of TiO_2 Nanostructures with CdS Quantum Dots. Particulate *versus* Tubular Support Architectures. *Adv. Funct. Mater.* **2009**, *19*, 805–811.
33. Lee, H.; Leventis, H. C.; Moon, S. J.; Chen, P.; Ito, S.; Haque, S. A.; Torres, T.; Nuesch, F.; Geiger, T.; Zakeeruddin, S. M.; *et al.* PbS and CdS Quantum Dot-Sensitized Solid-State Solar Cells: "Old Concepts, New Results". *Adv. Funct. Mater.* **2009**, *19*, 2735–2742.
34. Braga, A.; Gimenez, S.; Concina, I.; Vomiero, A.; Mora-Sero, I. Panchromatic Sensitized Solar Cells Based on Metal Sulfide Quantum Dots Grown Directly on Nanostructured TiO_2 Electrodes. *J. Phys. Chem. Lett.* **2011**, *2*, 454–460.
35. Lee, H.; Wang, M. K.; Chen, P.; Gamelin, D. R.; Zakeeruddin, S. M.; Gratzel, M.; Nazeeruddin, M. K. Efficient CdSe Quantum Dot-Sensitized Solar Cells Prepared by an Improved Successive Ionic Layer Adsorption and Reaction Process. *Nano Lett.* **2009**, *9*, 4221–4227.
36. Lee, H. J.; Yum, J. H.; Leventis, H. C.; Zakeeruddin, S. M.; Haque, S. A.; Chen, P.; Seok, S. I.; Gratzel, M.; Nazeeruddin, M. K. CdSe Quantum Dot-Sensitized Solar Cells Exceeding Efficiency 1% at Full-Sun Intensity. *J. Phys. Chem. C* **2008**, *112*, 11600–11608.

37. Huang, X. M.; Huang, S. Q.; Zhang, Q. X.; Guo, X. Z.; Li, D. M.; Luo, Y. H.; Shen, Q.; Toyoda, T.; Meng, Q. B. A Flexible Photoelectrode for CdS/CdSe Quantum Dot-Sensitized Solar Cells (QDSSCs). *Chem. Commun.* **2011**, *47*, 2664–2666.
38. Chi, C. F.; Cho, H. W.; Teng, H. S.; Chuang, C. Y.; Chang, Y. M.; Hsu, Y. J.; Lee, Y. L. Energy Level Alignment, Electron Injection, and Charge Recombination Characteristics in CdS/CdSe Cosensitized TiO_2 Photoelectrode. *Appl. Phys. Lett.* **2011**, *98*, 012101.
39. Lee, Y. L.; Lo, Y. S. Highly Efficient Quantum-Dot-Sensitized Solar Cell Based on Co-Sensitization of CdS/CdSe. *Adv. Funct. Mater.* **2009**, *19*, 604–609.
40. Kandilar, B.; Andreytc, R. Photovoltaic Effect in CdS−CdSe Heterojunctions. *Phys. Status Solidi* **1965**, *8*, 897–901.
41. Mahapatra, P. K.; Dubey, A. R. Photoelectrochemical Behavior of Mixed Polycrystalline n-Type CdS-CdSe Electrodes. *Sol. Energy Mater. Sol. Cells* **1994**, *32*, 29–35.
42. Kijitori, Y.; Ikegami, M.; Miyasaka, T. Highly Efficient Plastic Dye-Sensitized Photoelectrodes Prepared by Low-Temperature Binder-Free Coating of Mesoscopic Titania Pastes. *Chem. Lett.* **2007**, *36*, 190–191.